Influence of Peptide Composition, Gas-Phase Basicity, and Chemical Modification on Fragmentation Efficiency: Evidence for the Mobile Proton Model

Ashok R. Dongré,[§] Jennifer L. Jones,[†] Árpád Somogyi,[⊥,‡] and Vicki H. Wysocki*[,‡]

Contribution from the Department of Chemistry, Virginia Commonwealth University, Richmond, Virginia 23284-2006

Received December 19, 1995[⊗]

Abstract: Relative energetics of fragmentation of protonated peptides are investigated by using electrospray ionization/surface-induced dissociation (ESI/SID) tandem mass spectrometry. ESI/SID fragmentation efficiency curves (percent fragmentation versus laboratory collision energy) are presented for 20 oligopeptides and are a measure of how easily a peptide fragments. The relative positions of the ESI/SID fragmentation efficiency curves depend on several parameters which include peptide composition (e.g., presence/absence of a basic amino acid residue) and peptide size. The ESI/SID fragmentation efficiency curves, in combination with quantum chemical calculations, provide a unique approach to substantiate and refine the *mobile proton model* for peptide fragmentation. Selected peptides are also investigated to further test and confirm the mobile proton model; these include doubly-protonated peptides and chemically-modified peptides (i.e., acetylated and fixed-charge derivatized peptides). Doubly-protonated peptides fragment more easily than the singly-protonated forms of the same peptides, with a sequence dependence for the difference in energy required for the fragmentation of singly- vs doubly-protonated peptides. Acetylation at the amino terminus and arginine side chain leads to a decrease in basicity and a corresponding lower energy onset for fragmentation than for the unmodified form of the peptide. Fixing the site of charge by addition of trimethylammonium acetyl to the amino terminus, i.e., eliminating the mobile proton, results in a higher energy onset than that for the protonated form of the same peptide. Curves for doubly protonated peptides with two adjacent basic residues (Arg, Arg) suggest the localization of the two protons at the two basic side chains rather than at opposite termini of the peptide.

Introduction

The biological activity of peptides and proteins is directly correlated to their amino acid sequence and conformation. Unfortunately, detailed structural information for peptides and proteins in their native environment (i.e., in a "functional" cell) is difficult to obtain, so scientists rely mainly on structural data obtained *in vitro* in solutions or even in the solid phase. The most common methods used to study peptide structures and conformations in solution include circular dichroism (CD) and multidimensional NMR techniques.[1] X-ray crystallography is the method of choice to investigate solid-phase structures (which are quite similar to those in solution, because of water of crystallization).[2]

Since the early 1980s,[3] mass spectrometry has also been successfully used for structural investigation of peptides. With the development of "soft" ionization methods, such as liquid secondary ion mass spectrometry (LSIMS),[4] electrospray ionization (ESI),[5−9] and matrix assisted laser desorption (MALDI),[10,11] in combination with the development of tandem mass spectrometry (MS/MS),[12] the mass spectral investigation of large biomolecules is now accessible in many laboratories.

In addition to extensive and successful analytical applications of mass spectrometry for peptide sequencing, there have been substantial experimental[13−31] and theoretical[29,32−36] advancements in determination of energetics and mechanisms of peptide

* Author to whom correspondence should be addressed.

§ Current address: Department of Immunology, Howard Hughes Medical Institute, University of Washington, Seattle, WA 98195.

† Current address: Pharmaco LSR, 2240 Dabney Rd., Richmond, VA 23230.

⊥ On leave from the Central Research Institute for Chemistry of the Hungarian Academy of Sciences, P.O. Box 17, H-1525, Budapest, Hungary.

‡ Current address: Department of Chemistry, University of Arizona, Tucson, Az 85721.

⊗ Abstract published in *Advance ACS Abstracts,* August 15, 1996.

(1) (a) Styer, L. *Biochemistry*, 3rd ed.; W. H. Freeman & Co.: New York, 1988. (b) Nuclear Magnetic Resonance, Part C. In *Methods in Enzymology*; James, T. L., Oppenheimer, N. J., Eds.; Academic Press: New York, 1994; Vol. 239. (c) Biochemical Spectroscopy. In *Methods in Enzymology*; Sauer, K., Ed.; Academic Press: New York, 1995; Vol. 246.

(2) Drenth, J. *Principles of Protein X-ray Crystallography*; Springer-Verlag; New York, 1994.

(3) (a) Hunt, D. F.; Yates, J. R., III; Shabanowitz, J.; Winston, S.; Hauer, C. R. *Proc. Natl. Acad. Sci. U.S.A.* **1986**, *86*, 6233−6237. (b) Biemann, K.; Scoble, H. A. *Science* **1987**, *237*, 992.

(4) Fenselau, C.; Cotter, R. J. *Chem. Rev.* **1987**, *87*, 1−512.

(5) Dole, M.; Mack, L. L.; Hines, R. L.; Mobley, R. C.; Ferguson, L. D.; Alice, M. B. *J. Chem. Phys.* **1968**, *49*, 2240−2249.

(6) Fenn, J. B.; Mann, M.; Meng, C. K.; Wong, S. F.; Whitehouse, C. M. *Science* **1989**, *246*, 64−71.

(7) Mann, M.; Meng, C. K.; Fenn, J. B. *Anal. Chem.* **1989**, *61*, 1702−1708.

(8) Smith, R. D.; Loo, J. A.; Edmonds, C. G.; Barinaga, C. J.; Udseth, H. R. *Anal. Chem.* **1990**, *62*, 882−899.

(9) Smith, R. D.; Loo, J. A.; Barinaga, C. J.; Edmonds, C. G.; Udseth, H. R. *J. Am. Soc. Mass. Spectrom.* **1990**, *1*, 53−65.

(10) Karas, M.; Bachman, U.; Hillenkamp, F. *Int. J. Mass Spectrom. Ion Processes* **1987**, *78*, 53−81.

(11) Hillenkamp, F.; Karas, M.; Beavis, R. C.; Chait, B. T. *Anal. Chem.* **1991**, *63*, 1193A−1203A.

(12) Busch, K. L.; Glish, G. L.; McLuckey, S. A. Mass Spectrometry/Mass Spectrometry: Techniques and Applications of Tandem Mass Spectrometry; VCH Publishers: New York, 1988.

(13) Carr, S. A.; Hemling, M. E.; Bean, M. F.; Roberts, G. D. *Anal. Chem.* **1991**, *63*, 2802−2824.

(14) Biemann, K. *Methods Enzymol.* **1990**, *193*, 351−360, 455−479.

(15) Yost, R. A.; Boyd, R. K. *Methods Enzymol.* **1990**, *193*, 154−200.

(16) Gross, M. L. *Methods Enzymol.* **1990**, *193*, 131−153.

(17) Tomer, K. B. *Mass Spectrom. Rev.* **1989**, *8*, 445−482, 483−511.

(18) Biemann, K. *Biomed. Environ. Mass Spectrom.* **1988**, *16*, 99−111.

(19) (a) Hunt, D. F.; Henderson, R. A.; Shabanowitz, J.; Sakaguchi, K.; Michel, H.; Sevilir, N.; Cox, A. L.; Appella, E.; Engelhard, V. H. *Science* **1992**, *255*, 1261−1263. (b) Hunt, D. F.; Michel, H.; Dickinson, T. A.; Shabanowitz, J.; Cox, A. L.; Sakaguchi, K.; Appella, E.; Grey, H. M.; Sette, A. *Science* **1992**, *256*, 1817−1820.

S0002-7863(95)04219-3 CCC: $12.00

fragmentation and, to a more limited extent, conformations of protonated peptides in the gas phase. Biemann and co-workers have observed by high energy (keV) collision-induced dissociation (CID) that ions obtained by charge-remote fragmentation (namely **a**, **d**, and **w** ions) can predominate, and that the formation of these ions is related to the location of basic residues along the peptide backbone.[26,27] In contrast, the majority of the fragment ions observed by low-energy (eV) gas-phase or surface collisions are probably formed by charge-directed fragmentation pathways.[14,24,28,29,32] Deuterium labeling studies performed by Muller *et al*.,[37] Kenny *et al*.,[38] and more recently by Johnson *et al*.[39] suggest that rapid intramolecular proton transfers after gas-phase collisional activation yield a rapidly interconverting population of structures and induce charge-directed fragmentation pathways. These results are in agreement with deductions by Burlet *et al*.[40] and Tang *et al*.[41] for doubly-protonated peptides, where one proton is localized at the most basic site, and the second proton yields a heterogeneous population of structures resulting from rapid intramolecular proton transfers.

Surface-induced dissociation (SID), an ion activation method developed originally by Cooks and co-workers,[42] has proved to be a successful means to dissociate protonated peptides[29−31,43−49] and can provide sequence information for peptides including larger multiply charged peptides.[50,51] In addition, SID provides a controlled and relatively narrow internal energy distribution to the projectile ion,[52−54] which, together with the relatively cold ion formation by ESI, provides a unique experimental tool (ESI/SID) to study *relative* energetics of peptide fragmentation.[31]

In a recent communication to this journal,[31] we have shown that the ESI/SID onset energies for fragmentation of peptide ions depend on the presence or absence of a basic amino acid residue in the peptide (i.e., peptides with basic amino acid groups have higher fragmentation onsets than peptides devoid of basic amino acid groups). This suggests that a population of one dominant form of the protonated peptide (for peptides containing basic amino acid residues) exits the ESI source, and activation of this population then leads to proton transfers to less basic sites causing fragmentation of the peptide.[31]

In the work reported here, we extend our investigation of the energetics of peptide dissociation and the dependence of the relative energetics on peptide size, composition, and sequence. The relative positions of ESI/SID fragmentation efficiency curves are obtained for several types of peptides with different amino acid compositions and sequences (see Table 1). The relative shifts of the ESI/SID fragmentation efficiency curves within a series of peptides, where the peptide sequence and degrees of freedom are systematically altered, provide an experimental basis for substantiating and refining a model which we describe here as the "mobile proton model". This model is consistent with results and ideas published by many authors[27−32,37−41] and describes peptide dissociation as resulting from charge-directed cleavages that are initiated by intramolecular proton transfers. Relative energetic data and bond orders obtained by quantum mechanical calculations[29,32] are also incorporated into the mobile proton model. Additional experiments designed specifically to test the validity of the mobile proton model have been carried out and the results are presented. Comparison of results for doubly-protonated peptides with two basic residues positioned either adjacent to each other or at opposite termini suggests that the ESI/SID fragmentation efficiency curves can even be used to predict the sites of proton "localization" prior to activation and dissociation.

Experimental Section

The instrument used in these experiments is a tandem mass spectrometer specifically designed for low-energy ion-surface collisions.[55] The protonated peptides were formed by electrospray ioniza-

(20) Bean, M. F.; Carr, S. A.; Thorne, G. C.; Reilley, M. H.; Gaskell, S. J. *Anal. Chem.* **1991**, *63*, 1473−1481.
(21) Wysocki, V. H. In *Proceedings of the NATO Advanced Study Institute on Mass Spectrometry in the Biological Sciences: A Tutorial*; Gross, M. L., Ed.; Kluwer Academic Publishers: Hingham, MA, 1992; pp 59−77.
(22) Alexander, A. J.; Thibault, P.; Boyd, R. K.; Curtis, J. M.; Rinehart, K. L. *Int. J. Mass Spectrom. Ion Processes* **1990**, *98*, 107−134.
(23) Poulter, L.; Taylor, L. C. E. *Int. J. Mass Spectrom. Ion Processes* **1989**, *91*, 183−197.
(24) Ballard, K. D.; Gaskell, S. J. *Int. J. Mass Spectrom. Ion Processes* **1991**, *111*, 173−189.
(25) Biemann, K.; Martin, S. A. *Mass Spectrom. Rev.* **1987**, *6*, 1−75.
(26) Johnson, R. S.; Martin, S. A.; Biemann, K.; Stults, J. T.; Watson, J. T. *Anal. Chem.* **1987**, *59*, 2621−2625.
(27) Johnson, R. S.; Martin, S. A.; Biemann, K. *Int. J. Mass Spectrom. Ion Processes* **1988**, *86*, 137−154.
(28) Alexander, A. J.; Thibault, P.; Boyd, R. K. *Rapid Commun. Mass Spectrom.* **1989**, *3*, 30−35.
(29) McCormack, A. L.; Somogyi, Á.; Dongré, A. R.; Wysocki, V. H. *Anal. Chem.* **1993**, *65*, 2859−2872.
(30) Wysocki, V. H.; Jones, J. L.; Dongré, A. R.; Somogyi, Á.; McCormack, A. L. *Biological Mass Spectrometry: Present and Future*; John Wiley and Sons Ltd: New York, 1994, Chapter 2.14, pp 249−254.
(31) Jones, J. L.; Dongré, A. R.; Somogyi, Á.; Wysocki, V. H. *J. Am. Chem. Soc.* **1994**, *116*, 8368−8369.
(32) Somogyi, Á.; Wysocki, V. H.; Mayer, I. *J. Am. Soc. Mass Spectrom.* **1994**, *5*, 704−717.
(33) (a) Wu, J.; Lebrilla, C. B. *J. Am. Chem. Soc.* **1993**, *115*, 3270−3275. (b) Wu, J.; Lebrilla, C. B. *J. Am. Soc. Mass Spectrom.* **1995**, *6*, 91−101. (c) Wu, J.; Gard, E.; Bregar, J.; Green, M. K.; Lebrilla, C. B. *J. Am. Chem. Soc.* **1995**, *117*, 9900−9905.
(34) Zang, K.; Zimmerman, D. M.; Chung-Philips, A.; Cassady, C. J. *J. Am. Chem. Soc.* **1993**, *115*, 10812−10822.
(35) Zang, K.; Cassady, C. J.; Chung-Philips, A. *J. Am. Chem. Soc.* **1994**, *116*, 11512−11521.
(36) Bliznyuk, A. A.; Schaefer, H. F., III; Amster, I. J. *J. Am. Chem. Soc.* **1993**, *115*, 5149−5154.
(37) Mueller, D. R.; Eckersley, M.; Richter, W. J. *Org. Mass Spectrom.* **1988**, *23*, 217−222.
(38) Kenney, P. T.; Nomoto, K.; Orlando, R. *Rapid Commun. Mass Spectrom.* **1992**, *6*, 95−97.
(39) Johnson, R. S.; Krylov, D.; Walsh, K. A. *J. Mass Spectrom.* **1995**, *30*, 386−387.
(40) Burlet, O.; Orkiszewski, R. S.; Ballard, K. D.; Gaskell, S. D. *Rapid Commun. Mass Spectrom.* **1992**, *6*, 658−662.
(41) Tang, X-J.; Thibault, P.; Boyd, R. K. *Anal Chem.* **1993**, *65*, 2824−2834.
(42) Mabud, MD. A.; Dekrey, M. J.; Cooks, R. G. *Int. J. Mass Spectrom. Ion Processes* **1985**, *67*, 285−294. (b) Cooks, R. G.; Ast, T.; Mabud, MD. A. *Int. J. Mass Spectrom. Ion Processes* **1990**, *100*, 209−265.
(43) Bier, M. E.; Schwartz, J. C.; Schey, K. L.; Cooks, R. G. *Int. J. Mass Spectrom. Ion Processes* **1990**, *103*, 1−19.
(44) Aberth, W. *Anal. Chem.* **1990**, *62*, 609−611.
(45) (a) Williams, E. R.; Henry, K. D.; McLafferty, F. W.; Shabanowitz, J.; Hunt, D. F. *J. Am. Soc. Mass Spectrom.* **1990**, *1*, 413−416. (b) Chorush, R. A.; Little, D. P.; Beu, S. C.; Wood, T. D.; McLafferty, F. W. *Anal. Chem.* **1995**, *67*, 1042−1046.
(46) Wright, A. D.; Despeyroux, D.; Jennings, K. R.; Evans, S.; Riddoch, A. *Org. Mass Spectrom.* **1992**, *27*, 525−526.
(47) Cole, R. B.; LeMeillour, S.; Tabet, J.-C. *Anal. Chem.* **1992**, *64*, 365−371.
(48) McCormack, A. L.; Jones, J. L.; Wysocki, V. H. *J. Am. Soc. Mass Spectrom.* **1992**, *3*, 859−862.
(49) Schey, K. L.; Durkin, D. A.; Thornburg, K. R. *J. Am. Soc. Mass Spectrom.* **1995**, *6*, 257−263.
(50) (a) Wysocki, V. H.; Dongré, A. R. *Large Ions: Their Vaporization, Detection and Structural Analysis*; John Wiley & Sons Ltd., in press. (b) Dongré, A. R.; Somogyi, Á.; Wysocki, V. H. *43rd Proceedings of the American Society of Mass Spectrometry*, Atlanta, 1995; p 353.
(51) Dongré, A. R.; Somogyi, Á.; Wysocki, V. H. *J. Mass Spectrom.* **1996**, *31*, 339−350.
(52) Dekrey, M. J.; Kenttämaa, H. I.; Wysocki, V. H.; Cooks, R. G. *Org Mass Spectrom.* **1986**, *21*, 193−195.
(53) (a) Morris, M.; Riederer, D. E., Jr.; Cooks, R. G.; Ast, T.; Chidsey, C. E. D. *Int. J. Mass Spectrom. Ion Processes* **1992**, *122*, 181−217. (b) Miller, S. A.; Riederer, D. E., Jr.; Cooks, R. G.; Cho, W. R.; Lee, H. W.; Kang, H. *J. Phys. Chem.* **1994**, *98*, 245−251.
(54) Vékey, K.; Somogyi, Á.; Wysocki, V. H. *J. Mass Spectrom.* **1995**, *30*, 212−217.

Table 1. List of Peptides Investigated[a]

peptide	sequence[b]	MW	DOF	E_i (eV)
leucine enkephalin	YGGFL	556	228	33.2
leucine enkephalin-Lys	YGGFL***K***	684	291	50.9
Lys-leucine enkephalin	***K***YGGFL	684	291	57.9
leucine enkephalin-Arg	YGGFL***R***	712	297	62.4
Arg-leucine enkephalin	***R***YGGFL	712	297	60.9
thymosin α_1 fragment 23−27	VEEAE	576	228	34.5
[Lys^{23}]-thymosin α_1 fragment 23−27	***K***EEAE	605	243	46.6
$[Ala]_5$	AAAAA	373	156	25.4
Pro-$[Ala]_4$	PAAAA	400	168	32.8
Lys-$[Ala]_4$	***K***AAAA	430	189	38.8
$[Ala]_4$-Lys	AAAA***K***	430	189	35.9
$[Ala]_2$-Lys-$[Ala]_2$	AA***K***AA	430	189	36.2
Arg-$[Ala]_4$	***R***AAAA	459	195	46.8
Lys-Tyr-$[Ala]_4$	***K***YAAAA	593	252	46.8
Tyr-$[Ala]_4$-Lys	YAAAA***K***	593	252	47.9
bradykinin fragment 2−7	PPGFSP	600	246	51.2
des-Arg^1 bradykinin	PPGFSPF***R***	904	375	78.8
des-Arg^9 bradykinin	***R***PPGFSPF	904	375	78.3
collagen-type peptide	GAAGAA	417	168	29.1
collagen-type peptide	GPAGPA	469	192	39.2

[a] Each peptide sequence is represented by the single letter codes for each of the amino acids. The molecular weight (MW), degrees of vibrational freedom (DOF), and the collision energy determined at the inflection point of the ESI/SID fragmentation efficiency curve (E_i (eV)) for the singly protonated peptides are also included. [b] The basic amino acid groups are denote by bold and italics.

tion. The electrospray design used in our laboratory is a modified version of the designs by Chowdhury *et al*.[56] and Papac *et al*.[57] In this experimental setup, analytes are sprayed at atmospheric pressure from a syringe needle (flow rate of 2 μL/min) held at 4.0 kV toward a metal capillary (120 V). Desolvation of the ion occurs in the capillary, which is held at a temperature of approximately 100 °C. The desolvated ions are directed toward a skimmer cone (90 V) and enter into the high-vacuum region of the mass spectrometer where mass analysis and detection are accomplished. The tandem mass spectrometer consists of two 4000 u Extrel quadrupoles positioned at 90° with a surface positioned at the intersection of the ion optical paths of the quadrupoles. A protonated peptide of interest is mass selected by the first quadrupole and allowed to collide with the surface at a particular laboratory collision energy. The product ions formed by the internal excitation and subsequent dissociation of the parent ions are then analyzed by the second quadrupole. The laboratory collision energy is determined by the potential difference between the ion source skimmer cone and the surface; for multiply-charged ions the potential difference must be multiplied by the number of charges.

The fragmentation efficiency curves were obtained by fitting a logistic curve to the data points, which consist of $\sum$(fragment ion intensities)/$\sum$(total ion intensities) vs collision energy. The inflection points determined by this fit for these fragmentation efficiency curves are tabulated for different peptides (E_i values in Table 1). Spectra were obtained over a range of collision energies with each energy repeated at least 3 times, and the data listed in all tables are an average of a minimum of 3 data sets.

The chemically modified surface is a self-assembled monolayer film of octadecanethiol on gold.[58,59] Gold surfaces (1000 Å of vapor deposited gold on silica obtained from Evaporated Metal Films, Ithaca, NY) are cleaned by placing the surfaces in an ozone-rich, chemically-reactive environment in a UV cleaner (UV-Clean, Boekel, Philadelphia, PA) for 12 min. Octadecanethiol (1 mM in ethanol) is allowed to react with the clean vapor deposited gold surface for 24 h; the surfaces are rinsed with six portions of ethanol prior to insertion into the instrument. For a more detailed description of surface preparation, see ref 59.

The following peptides (YGGFL, YGGFLK, YGGFLR, VEEAE, KEEAE, PPGFSP, PPGFSPFR, and RPPGFSPF) were obtained from Sigma (St. Louis, MO) and used without further purification. RYGGFL was synthesized by Genosys Biotechnologies, Inc. (The Woodlands, Texas), and used without further purification. Other peptides (KYGGFL, KAAAA, AAKAA, AAAAK, RAAAA, PAAAA, YAAAAK, KYAAAA, GAAGAA, GPAGPA, and N-acetyl KYAAAA) were synthesized by Dr. Ron Jasensky at the Macromolecular Structure Facility, University of Arizona (Tucson, AZ). All samples were dissolved in 1% acetic acid/water solution to make stock solutions of a concentration range of ca. 1400−2000 pmol/μL. These stock solutions were then diluted in a 1:1 (v:v) methanol:1% acetic acid solution to final concentrations of 30−50 pmol/μL.

Acetylation of des-Arg^9 bradykinin (RPPGFSPF) was carried out by dissolving 1 mg of peptide in 1 mL of pH 6.0 4-morpholineethanesulfonic acid buffer solution and reacting with a 10-fold molar excess of acetic anhydride for 15 min in an ice bath.[60] The resulting reaction mixture was allowed to regain room temperature prior to removing buffer salts on HPLC (C18 semipreparative column from Applied Biosystems, eluent composition: 80% water, 20% acetonitrile, and 0.25% trifluoroacetic acid). The collected acetylated peptide fraction was lyophilized, and the product was dissolved in 1:1 (v:v) methanol: 1% acetic acid solution at final concentrations of 60−80 pmol/μL. The same procedure was used to obtain diacetylated peptide except that the peptide was dissolved in pH 10 buffer solution to deprotonate both the N-terminus and arginine side chain.

To obtain N-terminal fixed charge {trimethylammonium acetyl (TMAA)} derivatized peptides, the peptides were iodocetylated using iodoacetic anhydride by following the above acetylation procedure.[60,61] To the lyophilized iodoacetylated peptide 500 μL of a 25 wt % solution of trimethylamine was added and allowed to react for 30 min. Methanol (500 μL) was then added to a 500-μL aliquot of reaction mixture and the derivatized peptide solution was electrosprayed without further purification.

Results and Discussion

I. ESI/SID Fragmentation Efficiency Curves for Singly-Protonated Peptides. ESI/SID fragmentation efficiency curves were previously presented for a series of leucine enkephalin analogs as a communication in this journal.[31] To investigate whether the trends observed for leucine enkephalin and its analogs hold for other peptides, additional series of peptides have now been investigated (see Table 1). Fragmentation efficiency curves are plots of percent fragmentation vs laboratory collision energy (see e.g., Figure 1 which is discussed below). The inflection point energy (E_i) for the fragmentation efficiency curve of each of the singly protonated peptides investigated is listed in Table 1. The inflection point energy (E_i) of a given fragmentation efficiency curve corresponds to a laboratory collision energy associated with approximately 50% fragmentation of the mass-selected precursor ion. Since the influences of peptide size and sequence on the energetics of dissociation have not previously been characterized, comparisons are made initially within series of peptides of related sequence and, for comparisons between series, for peptides with similar numbers of degrees of freedom. It is shown that a simple linear degrees of freedom (DOF) correction of inflection point energies allows

(55) Wysocki, V. H.; Ding, J.-M.; Jones, J. L.; Callahan, J. H.; King, F. L. *J. Am. Soc. Mass Spectrom.* **1992**, *3*, 27−32.
(56) Chowdhury, S. K.; Katta, V.; Chait, B. T. *Rapid Commun. Mass Spectrom.* **1990**, *4*, 81−87.
(57) Papac, D. I.; Schey, K. L.; Knapp, D. R. *Anal. Chem.* **1991**, *63*, 1658−1660.
(58) (a) Porter, M. D.; Bright, T. B.; Allara, D. L.; Chidsey, C. E. D. *J. Am. Chem. Soc.* **1987**, *109*, 3559−3568. (b) Laibinis, P. E.; Whitesides, G. M.; Allara, D. L.; Tao, Y.-T.; Parikh, A. N.; Nuzzo, R. G. *J. Am. Chem. Soc.* **1991**, *113*, 7152−7167. (c) Bryant, M. A.; Pemberton, J. E. *J. Am. Chem. Soc.* **1991**, *113*, 8284−8293. (d) Li, Y.; Huang, J.; McIver, R. T., Jr.; Hemminger, J. C. *J. Am. Chem. Soc.* **1992**, *114*, 2428−2432. (e) Ulman, A. *Chem. Rev.* **1996**, *96*, 1533−1554.
(59) Somogyi, Á.; Kane, T. E.; Ding, J.-M.; Wysocki, V. H. *J. Am. Chem. Soc.* **1993**, *115*, 5275−5283.
(60) Wetzel, R.; Halualani, R.; Stults, J. T.; Quan, C. *Bioconjugate Chem.* **1990**, *1*, 114−122.
(61) Stults, J. T.; Lai, J.; McCune, S.; Wetzel, R. *Anal Chem.* **1993**, *65*, 1703−1708.

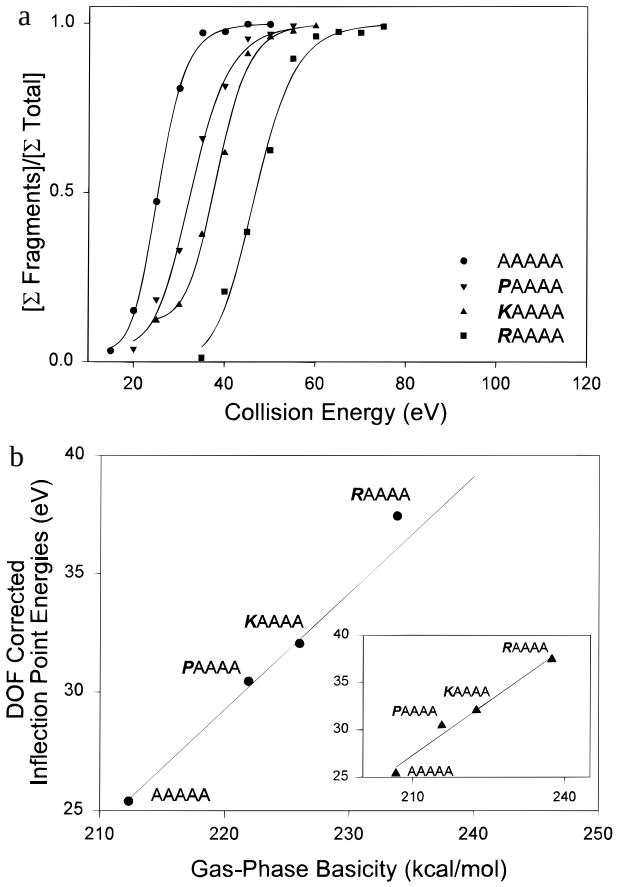

Figure 1. (a) Fragmentation efficiency curves of $[M + H]^+$ ions (ESI) for $[Ala]_5$ (AAAAA), Pro-$[Ala]_4$ (***P***AAAA), Lys-$[Ala]_4$ (***K***AAAA), and Arg-$[Ala]_4$ (***R***AAAA). The ions were formed by electrospray ionization and collided with an octadecanethiolate monolayer surface at a variety of collision energies (ESI/SID). The *y* axis represents Σ(fragment ion intensity)/Σ(total ion intensity) and the *x* axis represents SID collision energy. (b) A plot of DOF corrected laboratory collision energy at the inflection point (eV) versus gas-phase basicity (from ref 63) of the N-terminal amino acid residue for $[Ala]_5$ (AAAAA), Pro-$[Ala]_4$ (***P***AAAA), Lys-$[Ala]_4$ (***K***AAAA), and Arg-$[Ala]_4$ (***R***AAAA). The inset shows a similar plot, based on gas-phase basicities reported in refs 64, 65, and 66.

comparison between peptides of different size and sequence. Data for all these series of peptides are presented below and general trends are summarized. A peptide dissociation model that is consistent with the trends is described and compared with related work by other researchers.[27−32,37−41] Additional data specifically designed to test the model are presented and discussed.

We use here (see tables and figures) the laboratory collision energy, rather than average internal energy values, to characterize the position of the fragmentation efficiency curves. Peptide dissociation energetics are not known and thus the conversion of kinetic energy to internal energy (T → V) for peptides has not been characterized. Results for small projectile ions such as $W(CO)_6^{\bullet+}$, $Cr(CO)_6^{\bullet+}$, ferrocene, and benzene, however, yield (T → V) conversion of about 12−17%[54,55] on alkanethiolate monolayer surfaces and 18−28%[53,54] on fluorinated alkanethiolate monolayer surfaces. Although it has not been proven generally that these energy conversion values can be directly applied to larger ions such as protonated peptides, our preliminary results[62b] indicate that the (T → V) conversion values obtained for three pentapeptides (YGGFL, G_5, and A_5) are within the range reported for small ions colliding with an octadecanethiolate surface (10−20%).

Originally, a set of leucine enkephalin (YGGFL) analogs was chosen to represent peptides with no basic residues (YGGFL), with a basic residue at the carboxy C terminus (YGGFL***K*** and YGGFL***R***), and with a basic residue at the amino (N) terminus (***K***YGGFL and ***R***YGGFL). The inflection point energies of the appropriate SID fragmentation efficiency curves (Table 1) show that YGGFL has the lowest value within this series (33.2 eV collision energy), which indicates that protonated YGGFL fragments more easily at a given collision energy than related protonated peptides containing a basic residue (YGGFL***K***, ***K***YGGFL, YGGLF***R***, and ***R***YGGFL). Peptides containing lysine (YGGFL***K*** and ***K***YGGFL) have inflection points at lower energies than those containing arginine (YGGFL***R*** and ***R***YGGFL), which mimics the order of gas-phase basicities for lysine and arginine. An interesting shift is detected for ***K***YGGFL, a peptide which was synthesized and fragmented after publication of our earlier communication;[31] the fragmentation efficiency curve for ***K***YGGFL is shifted to higher collision energy (57.9 eV) than the fragmentation efficiency curve generated for YGGFL***K*** (50.9 eV). In contrast to this behavior for the lysine-containing leucine enkephalin analogs, the *position* of arginine in the peptides (***R***YGGFL and YGGFL***R***) does not significantly alter the onset energies for dissociation (60.9 and 62.4 eV, respectively). This is also the case for two other peptides that differ in the position of the arginine residue (***R***PPGFSPF and PPGFSPF***R***); these peptides give similar inflection point energies from their fragmentation efficiency curves (78.3 and 78.8 eV, respectively, Table 1). The fact that these two peptides (***R***PPGFSPF and PPGFSPF***R***) give different inflection point energies (78 eV) than the arginine-containing leucine enkephalins (61 eV for ***R***YGGFL and 62 eV for YGGFL***R***) is most likely a result of their larger number of degrees of freedom; i.e., molecules with more vibrational and rotational modes over which to distribute internal energy require higher energy input to fragment at the same rate as those with a smaller number of degrees of freedom. Our recent results for pentapeptide dimers and monomers suggest that a simple linear DOF correction is adequate for peptides of the size investigated here.[62] By using this linear correction, a DOF corrected inflection point energy (E_{DOF}) can be calculated from the following formula, $E_{DOF} = [DOF_{ref\ peptide}/DOF_{peptide}](E_i)_{peptide}$, where $DOF_{ref\ peptide}$ is number of degrees of freedom for the reference peptide, $DOF_{peptide}$ is the number of degrees of freedom for the peptide to which the simple DOF correction is to be applied, and $(E_i)_{peptide}$ is the inflection point energy of the peptide to which the DOF correction is to be applied.

Another peptide, VEEAE, that contains no basic group and has the same number of degrees of freedom as YGGFL has an inflection point value very close to that of YGGFL (34.5 eV vs 33.2 eV, Table 1). The substitution of lysine (K) instead of valine (V) leads to a significant increase in the inflection point value (see data for KEEAE in Table 1, 46.6 eV). Although the absolute value of the shift is a little bit smaller than that for the leucine enkephalin analogs, the qualitative trend for the shift between a nonbasic and lysine-containing peptide is the same.

To eliminate significant side chain and sequence effects, a set of synthetic alanine-containing peptides was investigated: AAAAA, PAAAA, KAAAA, and RAAAA. The fragmentation efficiency curves generated for these peptides are shown in Figure 1a. As the N-terminal amino acid residue is varied, differences in the onset energies for fragmentation are detected. The shifts detected for the curves are consistent with the order

(62) (a) Meot-Ner (Mautner), M.; Dongré, A. R.; Somogyi, Á.; Wysocki, V. H. *Rapid Commun. Mass Spectrom.* **1995**, *9*, 829−836. (b) Somogyi, Á.; Nair, H.; Wysocki, V. H.; Meot-Ner (Mautner), M. Manuscript in preparation.

of increasing gas-phase basicity of the N-terminal amino acid residue.[63] A plot of the DOF-corrected inflection point energy (the DOF correction is applied to the alanine analogs with AAAAA as the reference) for each peptide against the reported gas-phase basicity[63] of the amino acid residue substituted at the first position (N-terminal position) is presented in Figure 1b. Although a dependence between gas-phase basicity of the N-terminal amino acid residue and inflection point energy for the respective peptides is expected, it is interesting that a good *"linear"* fit is obtained for the first three points with a correlation coefficient of 0.99. The gas-phase basicity values used in Figure 1b were taken from the data presented by Amster and co-workers,[63] who used a bracketing technique to predict the gas-phase basicity of the 20 common amino acids. The fact that only arginine falls off the line is logical because Amster and co-workers[63] report a lower limit gas-phase basicity value for arginine (233.8 kcal/mol); an upper limit could not be predicted as there was no appropriate compound that did not react with arginine to transfer a proton. Recent gas-phase basicities reported for lysine (K)[64] and arginine (R)[65] by Fenselau and co-workers in combination with gas-phase basicity values for alanine and proline compiled by Lias and co-workers[66] also allow a good linear fit (see Figure 1b inset) between the DOF corrected inflection point energies and gas-phase basicities of the N-terminal amino acid residue for this set of synthetic alanine-containing peptides.

As mentioned earlier, there is a significant shift in the fragmentation efficiency curves between YGGFL***K*** and ***K***YGGFL. To confirm whether the *position* of the lysine influences the peptide fragmentation onsets, fragmentation efficiency curves were obtained for a set of synthetic peptides containing alanine and lysine (***K***AAAA, AA***K***AA, AAAA***K***, YAAAA***K***, ***K***YAAAA). The ESI/SID fragmentation efficiency curves for AAAA***K*** and AA***K***AA overlap (36 eV); however, the curve for ***K***AAAA is shifted to a slightly higher laboratory collision energy onset (39 eV). However, for YAAAA***K*** and ***K***YAAAA, only a 1-eV shift is observed in the position of the fragmentation efficiency curves. The placement of the lysine at the N-terminus of the peptide does shift the curve to higher onsets than onsets for peptides with lysine placed elsewhere. However, the magnitude of the shift is dependent on the peptide sequence. Further work is required to determine whether differences in secondary structure or a proton bridged form involving the lysine side chain[36] contribute to the different values for the shifts.

On careful observation of the inflection point energies for all the lysine-containing peptides regardless of the position of lysine along the backbone (see Table 2), it is evident that there is an increase in inflection point energy with increase in size of the peptides; this can be attributed to a mass effect, i.e., an increase in the number of degrees of freedom (DOF). The experimental inflection point values range from 35.9 to 57.9 eV. Upon application of the simple linear DOF correction, the corrected inflection point energies converge to values between 35 and 39 eV (see Table 2). As an example, the product of the inflection point energy for YAAAAK and the DOF ratio of AAAAK to YAAAAK yields a corrected inflection point energy for YAAAAK ($46.8 \times 189/252 = 35.1$ eV) with reference to AAAAK. A similar correction can be applied to arginine-containing peptides and yields corrected inflection point energies of 40 eV (see Table 2). It is likely that the simple linear DOF correction leads to over corrections of inflection point energies (e.g., compare values for the peptide used as the reference (**R**AAAA) to the corrected values in Table 2).

Table 2. List of Lysine- and Arginine-Containing Peptides Investigated Including the Sequence,[a] Degrees of Freedom (DOF), Inflection Point Energies,[b] and DOF Corrected Inflection Point Energies[c]

sequence[a]	DOF	inflection point energy, E_i (eV)[b]	DOF corr inflection point energy, E_{DOF} (eV)[c]
Lysine-Containing Peptides			
AAAA***K***	189	35.9	35.9
KAAAA	189	38.8	38.8
AA***K***AA	189	36.2	36.2
KEEAE	243	46.6	36.2
YAAAA***K***	252	46.8	35.1
KYAAAA	252	47.9	35.9
YGGFL***K***	291	50.9	33.1
KYGGFL	291	57.9	37.6
Arginine-Containing Peptides			
RAAAA	195	46.8	46.8
RYGGFL	297	60.9	39.9
YGGFL***R***	297	62.4	40.9
RPPGFSPF	375	78.3	40.7
PPGFSPF***R***	375	78.8	40.9

[a] The basic amino acid groups are denoted by bold and italics. [b] The inflection point energy value (E_i) is the collision energy at the inflection point for the ESI/SID fragmentation efficiency curves. [c] The DOF corrected inflection point energy (E_{DOF}) is calculated according to the formula $E_{DOF} = [DOF_{ref}/DOF_{peptide}]E_{i,peptide}$ (e.g., DOF corrected inflection point for YGGFL***K*** with respect to AAAA***K*** is $50.9 \times (189/291)$). Values for lysine-containing peptides are corrected to AAAA***K*** because this is the lysine-containing peptide with the smallest number of DOF and the smallest inflection point energy. Values for arginine-containing peptides are likewise corrected to ***R***AAAA.

Table 3. List of Non-Basic Residue-Containing Peptides Investigated Including the Sequence, Degrees of Freedom (DOF), Inflection Point Energies, E_i,[a] and DOF Corrected Inflection Point Energies, E_{DOF}[b]

sequence	DOF	inflection point energy, E_i (eV)[a]	DOF corr inflection point energy, E_{DOF} (eV)[b]
AAAAA	156	25.4	25.4
GAAGAA	168	29.1	27.0
YGGFL	228	33.2	22.7
VEEAE	228	34.5	23.6

[a] The inflection point energy value is the collision energy at the inflection point for the fragmentation efficiency curves. [b] The DOF corrected inflection point energy is calculated according to the formula $[DOF_{AAAAA}/DOF_{peptide}]E_{i,peptide}$ (e.g., DOF corrected inflection point for YGGFL with respect to AAAAA is $33.2 \times (156/228)$).

Another example of the mass effect is the relative positions of the curves for peptides with no basic residues but having different sequence and size. The experimental inflection point energy for VEEAE, which has exactly the same number of degrees of freedom as YGGFL, is very close to that of the YGGFL (34.5 vs 33.2 eV, Table 3). The position of the curve obtained for protonated $[Ala]_5$ which has a lower number of degrees of freedom is, however, significantly lower than that measured for YGGFL (25.4 eV vs 33.2 eV, Table 3). Neither peptide has a basic residue, so it is reasonable to assume that this difference is primarily due to their difference in size (mass effect). The corrected inflection point energy for YGGFL (i.e. product of inflection point energy of YGGFL and the DOF ratio of AAAAA to YGGFL) is 22.7 eV; a similar correction when applied to VEEAE yields a corrected inflection point energy of 23.6 eV (see Table 3). Furthermore, a similar correction can be applied to GAAGAA and the DOF corrected value is 27.0 eV. In contrast, GPAGPA, a peptide containing no basic side chains but two internal prolines, has a DOF corrected inflection

(63) Gorman, G. S.; Speir, J. P.; Turner, C. A.; Amster, I. J. *J. Am. Chem. Soc.* **1992**, *114*, 3986−3988.
(64) Wu, Z.; Fenselau, C. *Rapid Commun. Mass Spectrom.* **1994**, *8*, 777−780.
(65) Wu, Z.; Fenselau, C. *Rapid Commun. Mass Spectrom.* **1992**, *6*, 403−405.
(66) Lias, S. G.; Liebmann, L. F.; Levin, R. D. *J. Phys. Chem. Ref Data* **1984**, *13*, 695−808.

point energy which is higher than that observed for GAAGAA (32 eV vs 27 eV). Similarly, PPGFSP, a peptide containing a terminal proline and two internal prolines, has a DOF corrected inflection point energy (corrected with respect to PAAAA as reference) which is slightly higher than that observed for PAAAA (35 eV vs 33 eV). These results suggest that the presence of internal prolines, which are known to generate β-turns in a peptide chain, makes the fragmentation more demanding energetically. Further experimental and theoretical investigations of the proline effect are in progress in our laboratory.[67]

The inflection point energy data that are used to characterize the positions of ESI/SID fragmentation efficiency curves for the various singly charged peptides discussed above can be summarized as follows:

(i) After applying a linear correction for DOF (mass effect), comparison between series of peptides indicates that the shifts in fragmentation efficiency curves are mainly due to gas-phase basicity of the basic amino acid group present in the peptide. The presence and type of basic amino acid group along the peptide backbone dictates the energy requirement for fragmentation.

(ii) Peptides with no basic groups fragment at lower energies than those containing a basic residue.

(iii) The presence of a basic amino acid always increases the energy requirement for fragmentation. Within a series of peptides with similar structure, and also between series, the relative amount of shift correlates to the gas-phase basicity of the basic residue, i.e., arginine-containing peptides require higher energy to fragment compared to lysine-containing peptides, which in turn require higher energy to fragment than peptides containing no basic residues.

(iv) Internal prolines may have a unique effect; this could be due to the increased structural rigidity of the backbone making proton transfer (to yield a fragmenting structure) more sterically hindered thereby requiring higher energy to initiate fragmentation (see model below).

II. The Mobile Proton Model. By incorporating the ESI/SID experimental results presented above and results from our earlier quantum mechanical bond order calculations,[29,32] a model emerges that could explain the shifts detected in the ESI/SID fragmentation efficiency curves. For peptides, most of the common ion types observed by surface-induced dissociation (SID), low-energy collision-induced dissociation (CID), or photodissociation are rationalized as charge-directed fragmentation (cleavage occurs in the vicinity of a charge site, e.g., **b** ions), whereas charge-remote fragmentation (cleavage occurs remote to the site of charge) is generally dominant only under high-energy (keV) collision-induced dissociation of peptides with a basic residue (e.g., leading to a series of **a**, **d**, and **w** type ions).[27,68] For many of the peptides that we have investigated, the dominant ion types in the surface-induced dissociation spectra are those that are commonly rationalized as charge-directed cleavages. This means that different fragment ions in the spectra would have to result from different protonated forms of the same peptide, e.g., the location of the proton in a protonated molecule $[M + H]^+$ that fragments to a $\mathbf{b}_6$ ion would be different from the location of the proton in a protonated molecule that fragments to give a $\mathbf{b}_2$ ion, or a $\mathbf{y}_8$ ion, etc.

If protons were randomly located in the ions that leave the electrospray ion source and collide with the surface, without regard to whether or not basic residues are present in the molecule, then we could expect that peptides of similar size would have approximately the same onset energies for dissociation upon collision with the surface. This is not, however, consistent with the data presented above because the fragmentation efficiency curves depend dramatically on whether or not basic residues are present. On the other hand, if the ions leaving the electrospray ion source are internally "cold", then one stable form of a protonated peptide could dominate in the ion population that leaves the ion source. It is reasonable to assume that the proton is likely to be internally solvated. The internal solvation would involve different "pillar" atoms, such as the N of the amino terminus, the O of the amide group, the N of the amide group, or additionally, heteroatoms (N, O, S) of the side chain of an amino acid; see Scheme 1A. The relative contribution of the "most stable" protonated form to the total ion population would depend on the relative energy differences between this form and other less stable protonated forms. For peptides with no basic residue(s), the energies of the different proton-solvated forms are expectedly closer to each other than for peptides containing a basic residue. As a consequence, for a peptide with a basic amino acid, the relative contribution to the total ion population of a form protonated at the basic side chain would expectedly be high.

Important theoretical results were previously obtained based on *ab initio* and MNDO bond order and MNDO energy partitioning calculations.[29,32] The main conclusion of these calculations is that not all the protonated forms are fragmenting structures. *Ab initio* and MNDO bond order calculations clearly show that when the proton is located on the amide oxygen, the bond order of the amide bond is significantly greater (by 35−40%) relative to that of the unprotonated neutral. This suggests that the amide oxygen protonated form is not cleaved at the amide bond and is probably not a fragmenting structure. In contrast, when the proton is located on the amide nitrogen, the amide bond order is significantly smaller (by about 35%) than in the neutral, indicating a fragmenting structure (i.e., the cleavage of the amide bond in this form produces **b** ions). In general, bond weakenings or strengthenings track with the position of the proton at various sites along the peptide backbone as reflected clearly by bond order patterns.[32] An important additional note is that it is not necessary to locate the proton exclusively at one heteroatom. Even if the amide nitrogen is only partially involved in protonation (e.g., in a proton-bridged structure) it leads to weakening of the amide bond, however, to a lesser extent. Similarly, the amide bond is strengthened when the amide oxygen is involved in a H-bond formation.[29]

Based on the above experimental and theoretical results for singly charged peptides, a logical conclusion is that, regardless of the initial protonation site, the proton is finally transferred (exclusively or in a H-bond form) to less basic sites in the peptide via ion-activation. As a result, the population of protonated forms with higher energy than that of the most stable structure increases. Those structures in which the amide N is involved in protonation fragment more easily than other forms. It is important to emphasize that these protonated forms are not necessarily in thermal equilibrium, so their relative concentration cannot be calculated based strictly on their relative

(67) For example: Nair, H.; Somogyi, Á.; Wysocki, V. H. *J. Mass Spectrom*. In press.

(68) A protonated peptide upon collisional activation (CID or SID) leads to a host of sequence-specific fragment ions. If the charge is retained by the N-terminal portion of the peptide, ions are labeled as **a**, **b**, and **c** type ions; however, if the charge is retained by the C-terminal portion of the peptide then ions are labeled as **x**, **y**, and **z** type ions. In addition to backbone cleavage ions, side chain specific ions namely **d** and **w** type ions are also observed. For a more detailed description on sequence ions obtained upon collisional activation of a protonated peptide refer to the following publication: Biemann, K. *Biomed. Environ. Mass Spectrom.* **1988**, *16*, 99−111.

(69) Vékey, K.; Somogyi, Á.; Wysocki, V. H. *Rapid Commun. Mass Spectrom.* **1996**, *10*, 911−918.

Scheme 1

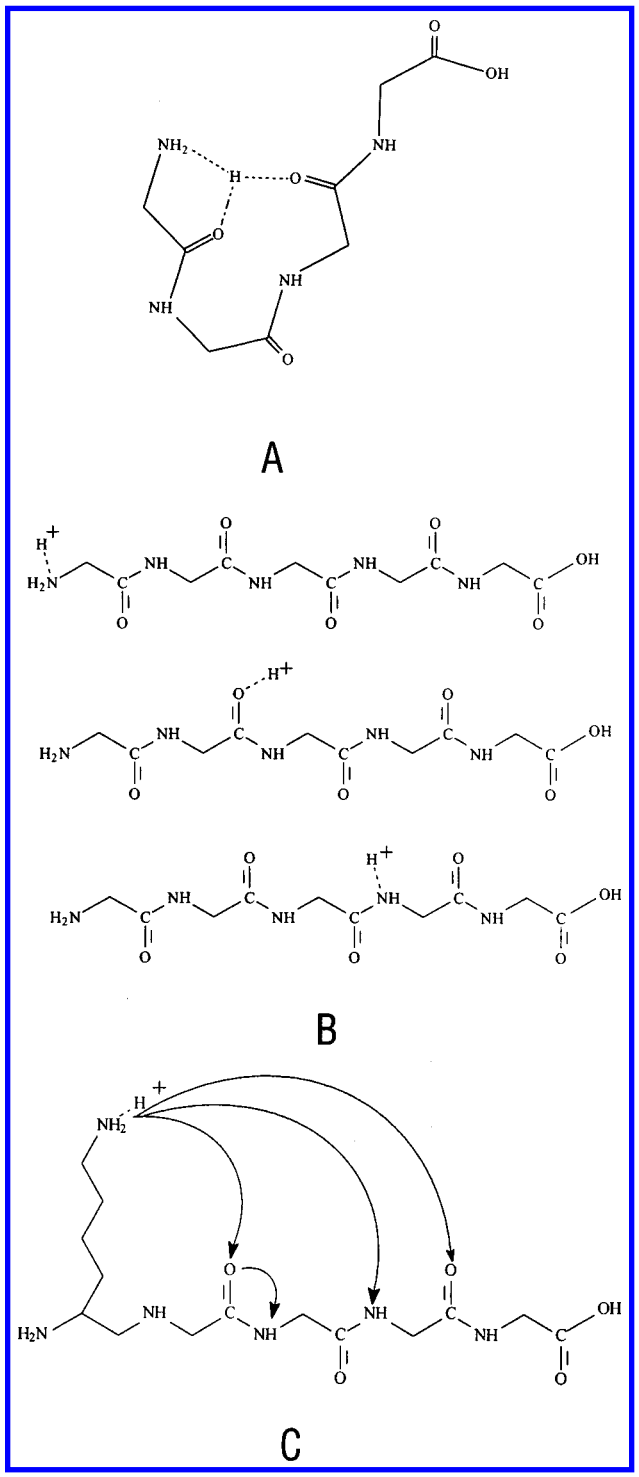

free energy values. Nevertheless, the fact that the relative shifts in fragmentation efficiency to higher collision energies can be correlated with increased gas-phase basicity of a peptide (e.g., arginine-containing peptides > lysine-containing peptides > peptides without a basic residue) clearly indicates the involvement of proton transfer in peptide fragmentation.

(a) Additional Comments—Internal Energy Requirements. Upon ion activation by surface collision, a large amount of internal energy is deposited to the protonated peptide. In our recent thermal decomposition studies,[62] we expressed the SID internal energy content as an "effective" SID temperature by comparing thermal dissociation rate constants to SID rate constants. For example, the SID activated protonated YGGFL is assigned equivalent temperatures of 710−840 K by extrapolation of the thermal activation (Arrhenius) parameters.[62a] Alternatively, by using average kinetic to internal energy conversion values obtained for small model systems (e.g., 17% which was obtained for benzene[54]), the internal energy supplied by the surface collision to protonated YGGFL is 33.2 eV × 0.17 = 5.6 eV at the inflection point of the fragmentation efficiency curve. By considering additional thermal excitation (occurring in the capillary of the electrospray source) and gas-phase collisional activation in the capillary-skimmer region, the average internal energy of $(YGGFL)H^+$ at the inflection point can be estimated as about 8 eV.[69] It is reasonable to assume that at these temperatures/internal energies rapid proton exchange along the peptide backbone can give rise to a heterogeneous population of protonated species (see Scheme 1). In other words, SID provides enough internal energy to mobilize the proton (that might originally be strongly solvated involving e.g., the side chain of a basic amino acid), leading to several protonated forms of the same peptide (see Scheme 1).

The internal energy required for proton mobilization to occur with a reasonable rate is influenced by the difference between the energy of the most stable form and the protonated form generated after proton mobilization. Another factor is the kinetic shift, the excess internal energy required to promote the reaction with a rate sufficient to be detected, which is influenced by the instrument used. For our SID instrument, the time scale for fragmentation is a few microseconds, so the internal energy must be sufficient to achieve a log k value of at least 6 for the proton transfer. A kinetic shift can cause even small differences in the proton transfer energy to result in detectable shifts in the SID collision energy scale. In general, it is difficult to measure the energy requirements for proton transfer from a more basic site to less basic sites. Recent model calculations[70] based on direct state counting show that the internal energy requirement to drive a reaction with a rate constant of 10^6 s^{-1} for a leucine enkephalin size (DOF = 228) peptide is 10.6 eV if the critical energy is 1.6 and 12.7 eV if the critical energy is 1.8 eV. (We use these critical energy values here because these are close to those reported recently, see, e.g., refs 62 and 71 and references therein. Also note that in both cases the same frequency factor of 10^{14} was used.) By using a T → V conversion factor of 17%, the difference in the above internal energy requirements (12.7−10.6 = 2.1 eV) corresponds to a shift of 2.1/0.17 = 12.3 eV in the SID collision energy scale. Although the estimated internal energy or SID energy shift is influenced by the frequency factor (i.e., these energies increase with decreasing frequency factors), the shift of 12.3 eV indicates that about a 0.2-eV difference in critical energy can be manifested in a well-detectable shift in the position of the ESI/SID fragmentation efficiency curves. In fact, the differences in the inflection point values of Table 1 range from a few to a few tens of electronvolts. Interestingly, the difference between the measured E_i values for two peptides of about the same size as YGGFL, VEEAE (nonbasic peptide with DOF = 228), and KEEAE (basic peptide, DOF = 243) is 12.1 eV.

(b) Additional Comments—Fragmentation Pathways. The extent to which the proton transfer competes with, or is preceded by, other pathways (e.g., NH_3 loss from a protonated arginine side chain or charge remote fragmentation) is not completey clear and varies with amino acid composition. Much additional research is required on detailed fragmentation mechanisms of

(70) Vékey, K., unpublished results obtained by using Christie's "RRKM Large" program: Derrick, P. J.; Loyd, P. M.; Cristie, J. R. In *Advances in Mass Spectrometry*; Cornides, I., Horváth, Gy., Vékey, K., Eds.; Wiley: Chichester, 1995; Vol. 13.

(71) (a) Rockwood, A. L.; Bushman, M.; Udseth, H. R.; Smith, R. D. *Rapid Commun. Mass Spectrom.* **1991**, *5*, 582. (b) Price, W. D.; Schnier, P. D.; Williams, E. R. *Anal. Chem.* **1996**, *68*, 859.

protonated peptides and the spectra for the systems investigated here provide a basis for our continued work in this area. (See refs 29, 50, and 51 for representative SID spectra from our laboratory.) In spite of the limited knowledge available on the detailed fragmentation mechanisms of these complex systems, the trends in fragmentation efficiency curves presented above are clear. Furthermore, many results and ideas consistent with the "mobile proton model" presented here have been published earlier in various forms.[27−32,37−41,67] In addition to our data presented above, further tests of the model are provided below for a variety of doubly charged and specifically chemically modified peptides. These systems provide additional strong evidence that initial proton localization depends on the type and number of basic residues present in a given peptide and that energy input is necessary for proton mobilization to induce dissociation.

III. Additional Experiments To Test the Mobile Proton Model. (a) Fragmentation Efficiency Curves of Derivatized Peptides (Acetylation and Fixed Charge Derivatization). Two types of derivatization were performed to test the mobile proton model. To further confirm whether proton localization and subsequent proton transfer are being monitored in these experiments, certain peptides were acetylated at the amino terminus and side chain to decrease the gas-phase basicity of the peptide (leading to a mixture of protonated forms of the same peptide). Another test to confirm whether proton localization plays a role in energetics of peptide dissociation is to fix the site of charge on the peptide; this would prevent transfer of charge (proton) along the peptide backbone and fragmentation would have to occur by another mechanism.

(i) Acetylation. If proton solvation is localized to a given part of the peptide (i.e., basic side chain), any modification to the peptide which increases the randomization of the proton location should be detected by an appropriate shift in the fragmentation efficiency curve. *Des*-Arg^9 bradykinin was chosen as a representative example to show the effect of mono- and diacetylation on ESI/SID fragmentation efficiency curves. In Figure 2a, the protonated form and monoacetylated form of *des*-Arg^9 bradykinin are illustrated to yield similar fragmentation efficiency curves with inflection point values of 78.3 and 78.2 eV, respectively (see Table 4) (note that the pH was monitored at 6.0 during the reaction to ensure that monoacetylation occurred at the amino terminus). A logical interpretation of these results is that the monoacetylated form can still be protonated on the arginine side chain, and the overall basicity of the peptide was not significantly altered by acetylation. Therefore, similar energies are necessary to transfer the proton from the basic site, the arginine side chain of des-Arg^9 bradykinin or N-amino mono acetylated des-Arg^9 bradykinin, to less basic sites, the amide nitrogen(s), to promote fragmentation. In contrast, diacetylation of *des*-Arg^9 bradykinin, which occurs at both the amino terminus and the arginine side chain, leads to a decrease in onset energy for fragmentation (see Table 4). In spite of the increase in mass (DOF), the shift to lower onset energy is consistent with a decrease in basicity leading, upon activation, to a mixture of protonated forms that fragment at lower collision energies relative to the unmodified *des*-Arg^9 bradykinin. With the simple DOF correction, the shift is even greater (see Table 4 for DOF corrected inflection point energies). Another example of the effect of diacetylation is shown in Figure 2b. Diacetylation of ***K***YGGFL also leads to a decrease in onset energy for fragmentation. Note that, in spite of their relative shift to lower energies, the fragmentation efficiency curves for the diacetylated derivatives still appear at relatively high collision energies (Figures 2a and 2b). This indicates that the proton may still be strongly solvated.

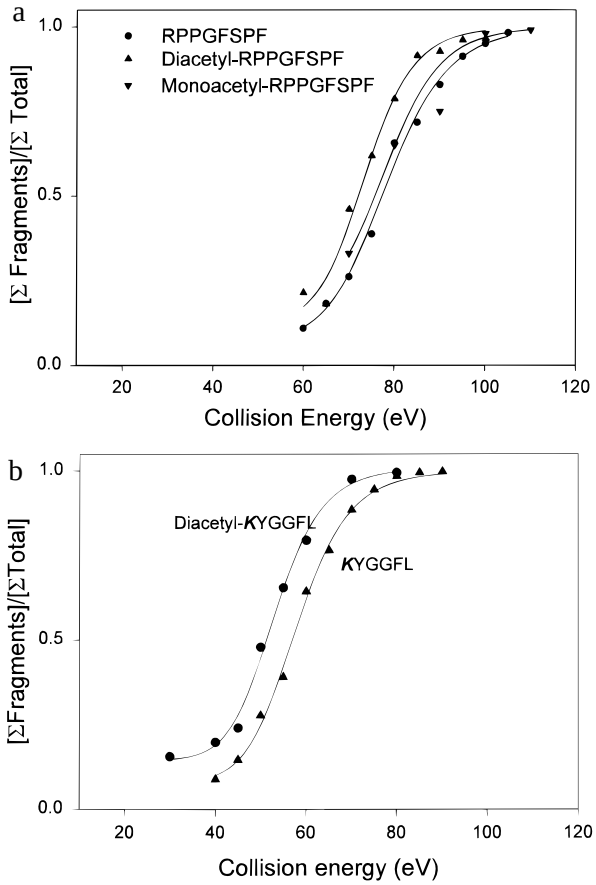

Figure 2. (a) Fragmentation efficiency curves (ESI/SID) of the [M + H]$^+$ ions for *des*-Arg^{9}bradykinin (***R***PPGFSPF) and its monoacetylated and diacetylated derivatives. The *y* axis represents Σ(fragment ion intensity)/Σ(total ion intensity) and the *x* axis represents SID collision energy. (b) Fragmentation efficiency curves (ESI/SID) of the [M + H]$^+$ ions for Lys-leucine enkephalin (***K***YGGFL) and its diacetylated derivative. The *y* axis represents Σ(fragment ion intensity)/Σ(total ion intensity) and the *x* axis represents SID collision energy.

Table 4. List of Non-Acetylated and Acetylated Peptides Including the Sequence, Degrees of Freedom (DOF), Inflection Point Energies, E_i (eV),[b] and DOF Corrected Inflection Point Energies, E_{DOF} (eV)[c]

sequence[a]	DOF	inflection point energy, E_i (eV)	DOF corr inflection point energy, E_{DOF} (eV)[c]
RPPGFSPF	375	78.3	78.3
monoacetyl-***R***PPGFSPF	390	78.2	75.1
diacetyl-***R***PPGFSPF	405	73.5	68.1
KYGGFL	291	57.9	57.9
diacetyl-***K***YGGFL	306	53.1	50.5

[a] The basic amino acid groups are denote by bold and italics. [b] The inflection point energy value, E_i, is collision energy at the inflection point for the fragmentation efficiency curves. [c] The DOF corrected inflection point energies are corrected with reference to ***R***PPGFSPF and ***K***YGGFL, respectively, e.g., the DOF corrected inflection point for monoacetyl-***R***PPGFSPF is 78.2×(375/390).

(ii) Fixed-Charge Derivatization. If intramolecular proton transfers from the most stable form of the peptide to less basic site(s) are necessary for fragmentation, then fixing the site of charge should also shift the position of the fragmentation efficiency curve. The fragmentation efficiency curves for protonated leucine enkephalin and an N-terminal fixed-charge derivatized form of leucine enkephalin are shown in Figure 3a. Fixing the site of charge by addition of "trimethylammonium

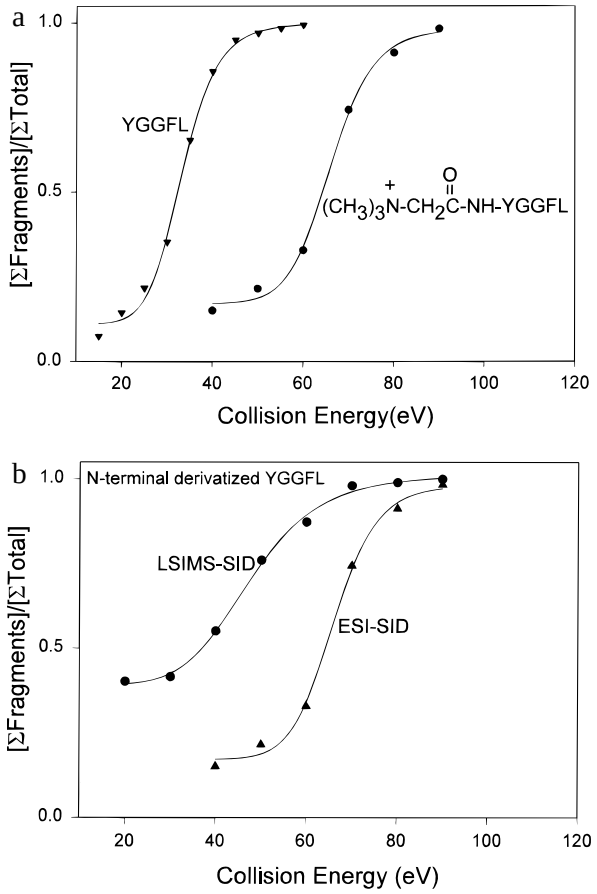

Figure 3. (a) Fragmentation efficiency curves (ESI/SID) of the $[M + H]^+$ ions of leucine enkephalin (YGGFL) and the fixed-charge derivatized form of leucine enkephalin. The *y* axis represents Σ(fragment ion intensity)/Σ(total ion intensity) and the *x* axis represents SID collision energy. (b) Comparison of fragmentation efficiency curves generated from surface-induced dissociation of ions formed by two different ionization method, LSIMS (Cs^+ bombardment) and electrospray for a fixed-charge derivatized form of leucine enkephalin. The *y* axis represents Σ(fragment ion intensity)/Σ(total ion intensity) and the *x* axis represents SID collision energy.

acetyl (TMAA)" to the amino terminus leads to a higher energy onset for fragmentation than that observed for protonated leucine enkephalin. This shift is expected since a fixed site of charge requires that fragmentation occur by charge-remote homolytic pathways which can require higher activation energies to produce backbone cleavage ions.[24]

Synthesis of the fixed-charge derivative also allowed us to further explore differences in average internal energy content deposited by the LSIMS and ESI ionization methods. We showed in our previous communication to this journal that the slopes and relative positions of the fragmentation efficiency curves depend dramatically on the ionization method used.[31] This has important implications for the interpretation of the data and for development of a general model for fragmentation of peptides. The fragmentation efficiency curves are much sharper (have steeper slopes) when the ion population is produced by ESI than if produced by (Cs^+ bombardment) LSIMS. Furthermore, the ESI conditions influence the position of the curves, with the lowest voltage difference between the capillary and skimmer leading to the highest measured onset energy for dissociation, i.e., the "colder" the ion population leaving the ion source, the greater the surface collision energy needed to dissociate the ions. This effect can be attributed to at least two different factors: (i) the ions leaving the electrospray ion source are of lower internal energy than those produced by LSIMS and/or (ii) different populations of structures (different mixtures of various protonated forms) are formed by the two methods. It is not possible to totally separate these effects for *protonated* peptides because higher internal energy content can lead to intramolecular proton transfers producing a mixture of structures. To eliminate one of these explanations, LSIMS/SID and ESI/SID fragmentation efficiency curves were obtained for the fixed-charge derivatized peptide (no proton present for intramolecular transfer).

Figure 3b shows ESI/SID fragmentation efficiency curves obtained for the N-terminal fixed-charge derivatized leucine enkephalin ionized by ESI and LSIMS ionization methods. The fragmentation efficiency curve for LSIMS-generated ions has a lower onset for fragmentation than that for ESI-generated ions. Also, the fragmentation efficiency curve obtained by LSIMS-generated ions is not as sharp, and the onset for the curve starts at a higher percent fragmentation than the curve obtained by ESI-generated ions. In contrast to *protonated* peptide ions generated by LSIMS or ESI where proton (charge) transfers are possible,[31] for fixed-charge derivatized peptides a mixture of different protonated forms cannot exist and, therefore, cannot contribute to the difference observed for the fragmentation efficiency curves. The difference can instead be attributed to a higher average internal energy content and a comparatively broader internal energy distribution for ions formed by LSIMS (6 keV Cs^+ bombardment) compared to ESI generated ions: greater SID collision energy is required to fragment the "colder" ions generated by ESI.

(b) Fragmentation Efficiency Curves of Doubly-Protonated Peptides. Another way to explore the "mobile" proton argument proposed in the model is to fragment doubly-protonated peptides.[21,22] One pair of peptides chosen for investigation is *des*-Arg^9 bradykinin (***R***PPGFSPF) and *des*-Arg^1 bradykinin (PPGFSPF***R***) because the amino acid composition and, as a consequence, the DOF values are identical: the only difference is the position of arginine. Fragmentation efficiency curves were obtained for the singly- and doubly-protonated forms of *des*-Arg^9 bradykinin and *des*-Arg^1 bradykinin and are represented in Figure 4a. For the singly-protonated forms of *des*-Arg^9 bradykinin, the ESI/SID fragmentation efficiency curves are almost identical (78.3 and 78.8 eV, Table 5); this can be explained by proton localization on the arginine side chain in either case. Addition of a second proton shifts fragmentation efficiency curves to lower energies for both peptides. The shift is more dramatic for *des*-Arg^9 bradykinin and a plausible explanation is that the first proton is located on the arginine side chain with the second proton expected to be more mobile, i.e., with the basic side chain protonated by the first proton, the remainder of the peptide would behave as a nonbasic peptide. This "mobile" proton allows charge directed cleavages and, as a result, less energy is needed to promote fragmentation. For *des*-Arg^1 bradykinin, the shift to lower onset energy for fragmentation of +2 vs +1 is not as dramatic as seen with *des*-Arg^9 bradykinin. The smaller shift for *des*-Arg^1 bradykinin can be explained on the basis that the first proton is located on the arginine side chain with the second proton localized at the next most basic site, the N-terminus. In this case, the N-terminus is a secondary amine (proline) and the proton would be expected to be held "more tightly" than if it were located at a primary amino terminus or randomly on the peptide backbone at amide O or N. As a result, a higher collision energy would be needed to promote the proton transfers necessary for fragmentation since the second proton is not "randomly" located as in the case of *des*-Arg^9 bradykinin.

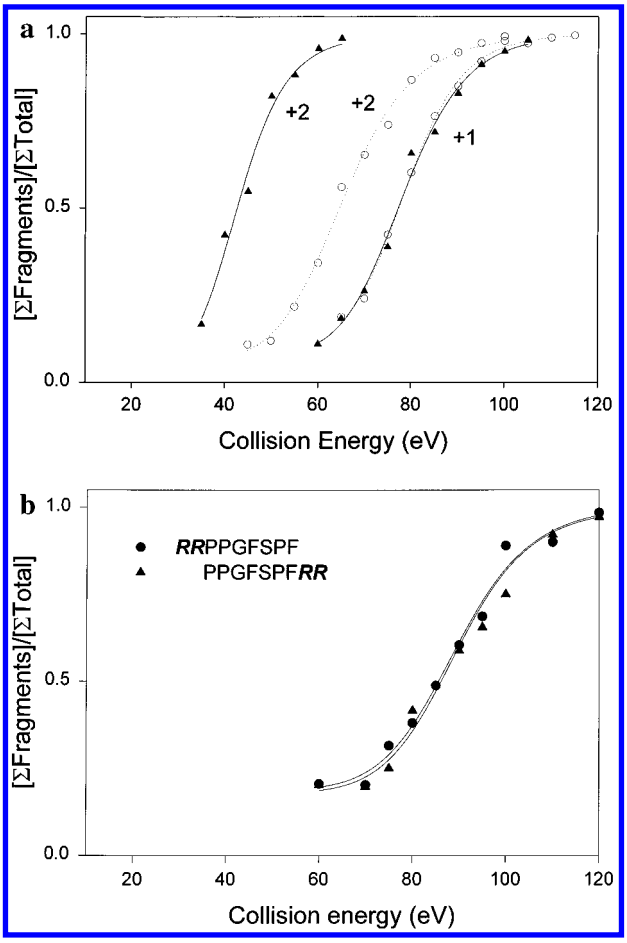

Figure 4. Fragmentation efficiency curves (ESI/SID) for the singly- and doubly-protonated forms of *des*-Arg[9] bradykinin (***R***PPGFSPF) (represented by ▲/−) and *des*-Arg[1] bradykinin (PPGFSPF***R***) (represented by ○/···). The *y* axis represents ∑(fragment ion intensity)/∑(total ion intensity) and the *x* axis represents SID collision energy. (b) Fragmentation efficiency curves (ESI/SID) for doubly-protonated forms of ***RR***PPGFSPF and PPGFSPF***RR***. The *y* axis represents ∑(fragment ion intensity)/∑(total ion intensity) and the *x* axis represents SID collision energy.

Table 5. List of Inflection Point Energies for Singly- and Doubly-Protonated Bradykinin Related Peptides Including the Inflection Point Energies for Singly- and Doubly-Protonated Peptides

sequence[a]	inflection point energy, E_i (eV) singly-protonated peptide	doubly-protonated peptide
RPPGFSPF	78.3	43.1
PPGFSPF***R***	78.8	65.5
RRPPGFSPF	*b*	89.3
PPGFSPF***RR***	*b*	92.5

[a] The basic amino acid groups are denote by bold and italics. [b] Singly-protonated peptide ions are not formed in the ESI source.

Another set of bradykinin-related peptides, namely ***RR***PPGFSPF and PPGFSPF***RR***, were also investigated. Fragmentation efficiency curves for the doubly-protonated ***RR***PPGFSPF and PPGFSPF***RR*** are represented in Figure 4b. The experimental inflection point energies for both these peptides, each of which contains two arginines, are shifted to considerably higher values (89.3 and 92.5 eV, respectively) compared to the doubly-protonated forms of *des*-Arg[9] bradykinin and *des*-Arg[1] bradykinin (see Table 5). If one proton was localized on one of the arginine side chains of ***RR***PPGFSPF, or bridged between the two arginine side chains, and the other proton was "mobile" over the backbone, the energy required to promote charge-directed cleavages should be similar to the experimental inflection point energy value for doubly-protonated *des*-Arg[9] bradykinin. However, the curve shifts to a considerably higher experimental inflection point energy on addition of the second arginine to the N-terminal side of *des*-Arg[9] bradykinin. This high onset energy can be attributed to localization of the two protons on the two arginine side chains. Another important observation is that fragmentation efficiency curves for doubly-protonated ***RR***PPGFSPF and PPGFSPF***RR*** overlap. These results indicate that, in the case of doubly-protonated PPGFSPF***RR***, the second proton is also preferentially "localized" at the second most basic site, i.e., the second arginine side chain, rather than at the other basic site along the backbone such as the N-terminal secondary amine (proline). These SID results clearly indicate that the charges are preferentially located at the most basic sites along the peptide backbone for these doubly-protonated peptide ions prior to collisional activation. These results are in agreement with recent results published by Biemann and co-workers,[72] who demonstrated by fragmentation patterns that two protons can reside in close proximity, overcoming the Coulombic repulsion which may be generated by the proximity of the charges.

Conclusions

The fragmentation efficiency curves obtained by electrospray ionization in combination with surface-induced dissociation (ESI/SID) (percent fragmentation of a given peptide as a function of laboratory collision energy) are a measure of how easily a protonated peptide fragments in the gas phase. We have demonstrated that the relative positions of these curves depend on the amino acid composition (e.g., absence or presence and type of a basic residue) and sequence, and the size of the peptide ("mass effect"). This dependence was established by studying the fragmentation of systematically chosen peptides, including chemically modified peptides (Table 1). Because a relatively narrow internal energy distribution is deposited by electrospray ionization coupled with surface-induced dissociation, ESI/SID is a unique and effective experimental tool for studying relative energetics of peptide fragmentation.

The ESI/SID fragmentation efficiency curves presented here for singly- and doubly-charged peptides provide a distinct experimental basis to further substantiate and refine the *mobile proton model* for peptide dissociation by tandem mass spectrometry. This model is also supported by quantum chemical calculations, and may possess a central role in the understanding of fragmentation of protonated peptides and their structural characteristics in the gas phase. The results described in this paper have increased our understanding of the mobile proton model to the extent where it can now serve as a *predictive* model to probe peptide dissociation and relative gas-phase basicities of oligopeptides.

Acknowledgment. This work was financially supported by a grant from the National Institute of Health (GM 51387).

JA9542193

(72) Downward, K. M.; Biemann, K. *J. Am. Soc. Mass Spectrom.* **1994**, *5*, 966−975.